

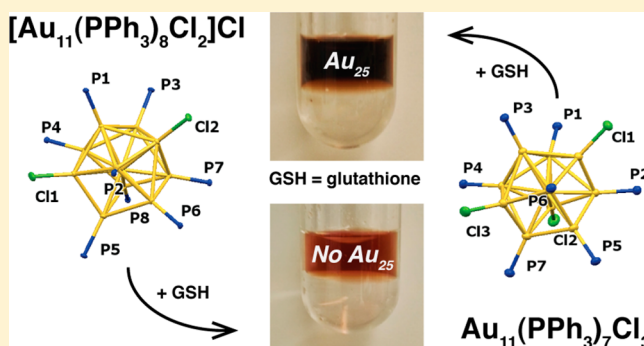
Structurally Similar Triphenylphosphine-Stabilized Undecagolds, $\text{Au}_{11}(\text{PPh}_3)_7\text{Cl}_3$ and $[\text{Au}_{11}(\text{PPh}_3)_8\text{Cl}_2]\text{Cl}$, Exhibit Distinct Ligand Exchange Pathways with Glutathione

Lallie C. McKenzie,^{†,‡} Tatiana O. Zaikova,[†] and James E. Hutchison*

Department of Chemistry and Biochemistry and Materials Science Institute, 1253 University of Oregon, Eugene, Oregon 97403-1253, United States

S Supporting Information

ABSTRACT: Ligand exchange is frequently used to introduce new functional groups on the surface of inorganic nanoparticles or clusters while preserving the core size. For one of the smallest clusters, triphenylphosphine (TPP)-stabilized undecagold, there are conflicting reports in the literature regarding whether core size is retained or significant growth occurs during exchange with thiol ligands. During an investigation of these differences in reactivity, two distinct forms of undecagold were isolated. The X-ray structures of the two forms, $\text{Au}_{11}(\text{PPh}_3)_7\text{Cl}_3$ and $[\text{Au}_{11}(\text{PPh}_3)_8\text{Cl}_2]\text{Cl}$, differ only in the number of TPP ligands bound to the core. Syntheses were developed to produce each of the two forms, and their spectroscopic features correlated with the structures. Ligand exchange on $[\text{Au}_{11}(\text{PPh}_3)_8\text{Cl}_2]\text{Cl}$ yields only small clusters, whereas exchange on $\text{Au}_{11}(\text{PPh}_3)_7\text{Cl}_3$ (or mixtures of the two forms) yields the larger Au_{25} cluster. The distinctive features in the optical spectra of the two forms made it possible to evaluate which of the cluster forms were used in the previously published papers and clarify the origin of the differences in reactivity that had been reported. The results confirm that reactions of clusters and nanoparticles may be influenced by small variations in the arrangement of ligands and suggest that the role of the ligand shell in stabilizing intermediates during ligand exchange may be essential to preventing particle growth or coalescence.



INTRODUCTION

Ligand exchange is a leading approach to functionalize inorganic nanoparticles and clusters. Exchange, or replacement, of the ligands used during synthesis with specific molecules or polymers introduces desired functionality onto the periphery of a nanoparticle for specific applications or scientific investigations.^{1,2}

Gold nanoparticles and clusters are among the most widely studied inorganic cores,³ yet the roles of the surface ligands are less understood. Most reports focus on either (i) the roles that ligands play during synthesis to control the size, shape, stability and solubility of nanoparticles or (ii) how ligands are used to introduce new functionality through ligand exchange.^{4–6} Few studies have been conducted to elucidate the mechanisms of exchange reactions^{7,8} or to probe the influence of the ligands on the nanoparticle reactivity.

Ligand exchange of thiols for triphenylphosphine is widely used to produce functionalized gold nanoparticles.^{2,9,10} Following on our discovery that larger ($d_{\text{core}} \sim 1.5$ nm) triphenylphosphine (TPP)-stabilized gold nanoparticles are excellent synthons to produce dozens of differently functionalized thiol-stabilized gold nanoparticles,^{9,11} we recognized that TPP-stabilized undecagold clusters might also serve as a building block to produce thiol-stabilized undecagold clusters

by ligand exchange. In the decades since their discovery in 1966,^{12–14} triarylphosphine-stabilized undecagold clusters have been of interest due to the optical and electronic properties that stem from the 11-atom Au core¹⁴ and their utility as heavy atom contrast agents for electron microscopy.^{15–17} A range of substituted triarylphosphines have been employed to introduce specific functionality to the cluster and/or to render the cluster water-soluble;^{15,17} however, exchanges with thiols had not been explored.

We showed that phosphine-to-thiol ligand exchange reactions on undecagold provide access to functionalized subnanometer clusters.^{10,18} Although TPP-stabilized undecagold is more inert than its larger analogs, ligand exchange proceeds smoothly at 55 °C¹⁹ with ~ 20 equiv of ligand per particle. Exchange can be carried out in organic solution or under biphasic conditions¹⁰ to produce functionalized clusters with the same small core size as the starting cluster. Given the broad range of available functionalities¹⁰ and the relative ease of synthesis, this approach has been used widely to produce functionalized clusters.^{14,20–23}

Received: July 24, 2014

Published: August 29, 2014

A key finding from our studies was that the small particle core size was retained during exchange.^{10,18} Thus, we were surprised to learn that others obtained different results when reportedly using the same approach. Shichibu et al. reported products of higher nuclearity (Au_{25}) were produced using a large excess (430 equiv) of glutathione in a biphasic ligand exchange.²⁰ Subsequently these authors reported that Au_{25} is also formed in partial ligand exchanges with 60 equiv of various alkylthiols in a single-phase (CHCl_3) exchange.²¹ The authors state that $\text{Au}_{11}(\text{PPh}_3)_8\text{Cl}_2^+$ is the major component within the starting undecagold cluster based upon optical spectra and ESI-MS. They attribute the formation of Au_{25} to the flocculation of higher nuclearity particles that are subsequently reduced in size (etched) in the presence of excess thiol. Yang and Chen reported that the use of the same undecagold synthesis²² produced $\text{Au}_{11}(\text{PPh}_3)_7\text{Cl}_3$ instead of $[\text{Au}_{11}(\text{PPh}_3)_8\text{Cl}_2]\text{Cl}$. They reported that the core size was preserved during exchange, although the optical spectra show the signature absorption of Au_{25} at 670 nm.²⁴ It has been suggested that these discrepancies in the literature are related to differences in characterization,^{21,25} reaction conditions (e.g., nitrogen vs air atmosphere),²⁰ or exchanging ligand identity;²⁶ however, the root cause remains unclear.

In an attempt to understand possible reasons for these differing reports, we examined the optical spectra of the precursor clusters reportedly used in different ligand exchanges. The absorption spectra of undecagold species have greater fine structure than in larger gold species, and the fine structure is sensitive to the core structure and ligand composition. A comparison of the optical spectra of the undecagold precursors reported in the literature is provided in Figure 1. Differences in the spectra suggest that different undecagold precursors were used, which might explain the disparate results obtained in the different laboratories.

A review of the literature revealed a number of reports of undecagold clusters possessing a variety of TPP-based ligands and different anions. There are a number of crystal structures

but almost no corroborating spectral data. To further compound the situation, “undecagold”, “ $\text{Au}_{11}(\text{PPh}_3)_7\text{Cl}_3$ ” and “ $\text{Au}_{11}(\text{PPh}_3)_8\text{Cl}_3$ ” have been used interchangeably (sometimes in the same publication) to refer to $\text{Au}_{11}(\text{PPh}_3)_n\text{Cl}_3$ clusters for which crystal structures or definitive spectral data were not available.^{10,15,16,18,21,22,27–29}

Herein, we report the first complete characterization of $\text{Au}_{11}(\text{PPh}_3)_7\text{Cl}_3$ (**Au11-7**) and $[\text{Au}_{11}(\text{PPh}_3)_8\text{Cl}_2]\text{Cl}$ (**Au11-8**) and the surprising discovery that the small differences in ligation result in dramatically different ligand exchange reactivity. Single crystal X-ray structures show that the two clusters have almost identical Au cores and vary only in the number of bound triphenylphosphine and chloride ligands. The two species have significantly different stabilities and reactivities. Analysis of the optical spectra shown in Figure 1 and the findings reported herein explain the disparate results that have been reported in the literature: under the conditions that we originally reported,^{10,18} ligand exchange of **Au11-8** yields clusters with the small core size, whereas the same exchanges of solutions containing **Au11-7** lead to aggregation and the production of Au_{25} .

RESULTS AND DISCUSSION

There Are Two Forms of “Triphenylphosphine-Stabilized Undecagold”. We previously demonstrated that $[\text{Au}_{11}(\text{PPh}_3)_8\text{Cl}_2]\text{Cl}$ (**Au11-8**) could be synthesized and employed in ligand-exchange reactions to produce more than 20 thiol-stabilized gold clusters based upon the undecagold core.¹⁰ Characterization by TEM, XPS and TGA confirmed the core size and ligand shell composition. Upon careful recrystallization from CH_2Cl_2 /hexanes,¹⁸ pure **Au11-8** can be prepared in ~20% yield as red plates that show a single set of three resonances in the aromatic region of the ^1H NMR.

During our attempts to produce larger quantities of **Au11-8**, we found that in some samples, the NMR spectra showed a second set of peaks in the aromatic region, the UV–visible absorbance spectra were less defined, and two types of crystals (red plates and orange needles) were produced. The two crystal forms were mechanically separated (Figure 2), redissolved, and characterized. Distinct NMR and UV–visible absorbance spectra confirmed that two unique molecular species had been isolated. The red plates had the same spectral features as **Au11-8**, (the precursor we used in our previous ligand-exchange experiments),^{10,18} while the other compound was a different cluster species.

X-ray quality crystals were grown for both forms in order to correlate the structures with their spectral features. Two unique structures containing TPP and chloride ligands were determined by crystallographic analysis. The orange needles were identified as $\text{Au}_{11}(\text{PPh}_3)_7\text{Cl}_3$ (**Au11-7**), and the red plates were **Au11-8** (Figure 2). The **Au11-7** structure shows that seven phosphines and three chlorides ligate all ten gold atoms on the surface of the cluster. In the **Au11-8** structure, an additional phosphine is bound to the surface, displacing one of the chlorides to an outer sphere position. The gold cores of the two clusters are nearly identical to each other and similar to previously identified undecagold clusters with different substitutions on the phosphine groups and a variety of anions.^{12,27,30–35} In addition, the bound phosphine and chloride ligands are located in the same positions as in previously determined $\text{Au}_{11}(\text{PPh}_3)_7\text{Cl}_3$ ³⁶ and $\text{Au}_{11}(\text{PPh}_3)_8\text{Cl}_3$ ³⁷ structures. Solution spectral data, including proton NMR, ^{31}P NMR, and UV–visible spectroscopy, were collected for each of

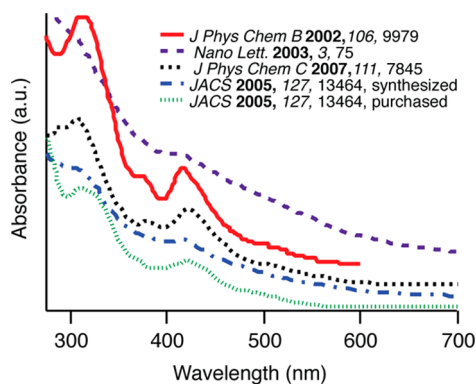


Figure 1. Optical spectra reported for TPP-stabilized undecagold clusters illustrating clear differences in peak positions (at approximately 300 and 420 nm), relative intensities of the peaks, and extent of fine structure for each example. All data were digitized from the cited sources, placed on the same scale, and offset in the vertical direction for clarity. Adapted with permission from Hutchison, J. E. et al. *J. Phys. Chem. B* **2002**, 106, 9979 (ref 18); Chen, S. et al. *Nano Lett.* **2003**, 3, 75 (ref 22); Shichibu, Y. et al. *J. Amer. Chem. Soc.* **2005**, 127, 13464 (ref 20); Shichibu, Y. et al. *J. Phys. Chem. C* **2007**, 111, 7845 (ref 21). Copyright 2002, 2003, 2005, and 2007 American Chemical Society.

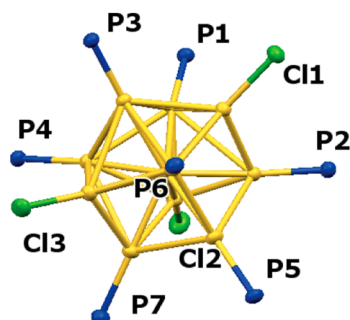
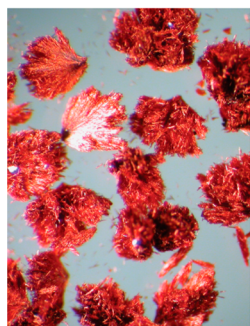
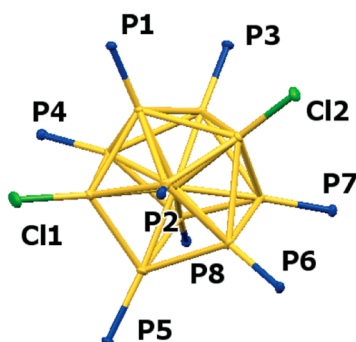
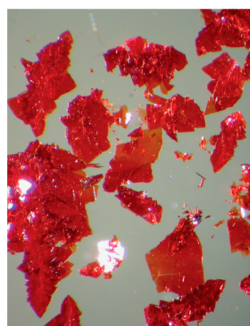
$\text{Au}_{11}(\text{PPh}_3)_7\text{Cl}_3$ (needles) $[\text{Au}_{11}(\text{PPh}_3)_8\text{Cl}_2]\text{Cl}$ (plates)

Figure 2. Optical micrographs and X-ray crystal structures of the central cores of the two crystalline forms of triphenylphosphine-stabilized undecagold. The needles (top) are composed of undecagold with seven phosphines in the ligand shell: $\text{Au}_{11}(\text{PPh}_3)_7\text{Cl}_3$. The plates (bottom) have been identified as undecagold with eight phosphines in the ligand shell and one outer sphere chloride: $[\text{Au}_{11}(\text{PPh}_3)_8\text{Cl}_2]\text{Cl}$. The two crystal structures have been oriented to illustrate that both have similar frameworks with the exception of the difference in chlorine ligation. The frameworks are shown with thermal ellipsoids given at the 30% probability level.

the structures, providing the first comprehensive comparison of two clusters, **Au11-7** and **Au11-8**, that contain the same phosphine and halide ligands but exhibit different ligand arrangements.

Although TEM is commonly used to determine the core size of metal nanoparticles, accurate measurement of subnanometer structures can be challenging due to limits in resolution and contrast. In addition, only the cores of metal nanoparticles can be imaged because TEM relies on the difference in contrast between high-Z and low-Z elements. Identical size distributions of 0.8 ± 0.3 nm were confirmed for both crystallized materials. TEM imaging cannot discriminate between the two forms; thus, other analytical techniques were employed as the primary characterization tools.

Each Form Has Distinct Spectral Signatures. Although NMR spectroscopy can rarely be used to identify specific structural forms of gold nanoparticles or clusters, it provides valuable structural information for the monodisperse cluster species in this study. NMR spectroscopy directly probes the ligand environments of nanoparticles and therefore provided opportunities to distinguish between the two Au_{11} clusters, as opposed to TEM. Each species can be readily identified in solution because the observed ^1H and ^{31}P NMR spectra (Figure 3A and Supporting Information) are uncomplicated and distinct. The data confirmed the previous spectral assignments

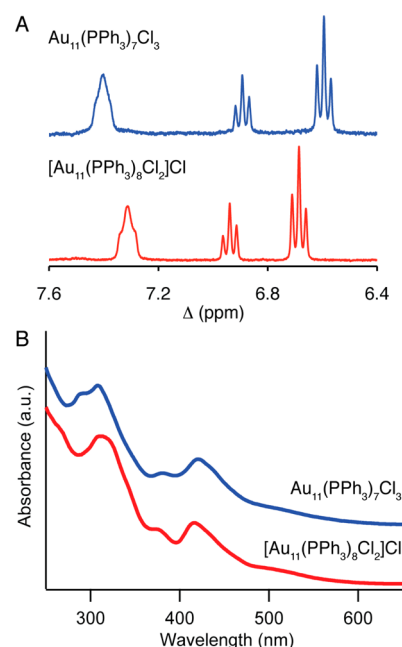


Figure 3. ^1H NMR and UV–visible spectra for the two pure triphenylphosphine-stabilized undecagold clusters recorded in CD_2Cl_2 and CH_2Cl_2 , respectively. In the ^1H NMR spectra (A), resonances for phenyl protons in the ligand shell of each form have diagnostic chemical shifts. The UV–visible spectra (B) show differences in the peak positions and intensities (see text for details). Compared to the spectra in Figure 1, each pure form shows well-defined spectral features.

for **Au11-8**¹⁸ and suggest that the two clusters have similar but not identical electronic structures.³⁸

The aromatic ring protons in the bound PPh_3 ligands of each Au_{11} cluster exhibit three distinct multiplet peaks with chemical shifts between 7.4 and 6.6 ppm that result from differential shielding of the protons in the ortho, meta, and para positions of the ligand upon binding to the metal.³⁹ The integration of the peaks matches the expected 2:2:1 ratio in both compounds. The larger downfield chemical shift for the ortho protons and larger chemical shift difference between peaks in the **Au11-7** spectra suggest that the electronic environment of the ligands in **Au11-7** is impacted by the Au core to a greater extent than in **Au11-8**. **Au11-7** also displays a larger downfield shift in the ^{31}P NMR data (see Supporting Information).

Spectral features can be definitively assigned to both structural forms. Spectra of pure **Au11-7** and **Au11-8** (obtained by dissolving the crystals of each form used for X-ray analysis) show distinct peaks and shoulders characteristic of undecagold clusters.⁴⁰ The presence of defined peaks, as opposed to the broader spectra often reported in the literature (for example in Figure 1), suggest that the crystalline samples have a higher degree of purity than samples exhibiting less-defined spectra. The data confirm our previous spectral assignments for **Au11-8**, including strong absorbances at 240, 312, and 416 nm.¹⁸ The peaks in the spectrum for **Au11-7** (at 420 and 308 nm) are shifted from those of **Au11-8**. Both of the peaks of **Au11-7** are accompanied by smaller peaks at shorter wavelengths. The absorbance bands for undecagold have been attributed to transitions in the $[\text{Au}_{11}]^{3+}$ core, and the differences in absorption wavelength for the two forms likely result from changes in the core geometry required to

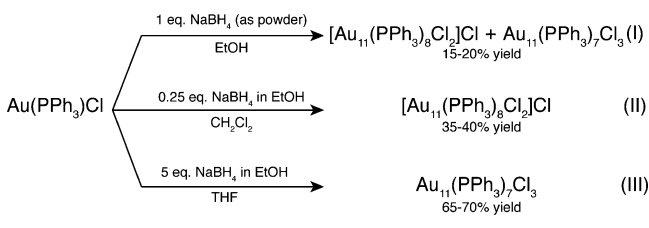
accommodate the additional bound phosphine in **Au11**–**8**.^{16,41,42}

Mixtures of the two clusters display broad absorbances in the UV–visible spectra, rather than the distinct peaks found in the pure clusters. In Figure 1, the spectrum of the material used in Hutchison et al. shows peaks at 312 and 416 nm. These wavelengths suggest that the starting material for ligand exchange in our initial studies¹⁸ was primarily **Au11**–**8**. On the other hand, the spectra from Yang and Chen²² and the synthesized material from Shichibu et al.²⁰ exhibit broad peaks. These spectra suggest that the starting materials in both ligand exchange reactions contained a mixture of clusters including both forms of TPP-stabilized undecagold. The spectra from Shichibu et al.²¹ and undecagold show distinct features, suggesting higher purity; however, the location of the peaks suggests that the materials used in these studies were primarily **Au11**–**7**.

Each of the Two Forms Can Be Readily Synthesized.

Once distinct spectral features could be assigned to the two clusters, we aimed to develop methods to directly synthesize each form. Phosphine-stabilized gold clusters are typically synthesized by reduction of mononuclear gold phosphine complexes with NaBH_4 .⁴³ In our previous work,^{10,18} AuPPh_3Cl was used as the starting material and was reduced with one molar equivalent of NaBH_4 in ethanol (Scheme 1). Under these

Scheme 1. New Syntheses of Pure $[\text{Au}_{11}(\text{PPh}_3)_8\text{Cl}_2]\text{Cl}$ and $\text{Au}_{11}(\text{PPh}_3)_7\text{Cl}_3$ Compared to the Preparation Typically Used to Prepare **Au11**



conditions, we observed formation of a mixture of two different undecagold species, but **Au11**–**8** was the primary product after crystallization. It was expected that by varying the reaction conditions, including the reagent ratios, solvents, and temperature, controlled routes to each form could be developed.

It has been reported that $[\text{Au}_{11}(\text{PPh}_3)_8\text{Cl}_2]^+$ can be synthesized through the conversion of $\text{Au}_9(\text{PPh}_3)_8(\text{NO}_3)_3$ ^{44,45} and that $\text{Au}_9(\text{PPh}_3)_8(\text{NO}_3)_3$ can be synthesized in ethanol with a 1:0.25 molar ratio of $\text{AuPPh}_3\text{NO}_3$ to NaBH_4 .⁴⁶ Based upon these findings, we explored whether decreasing the ratio of NaBH_4 to $\text{Au}(\text{PPh}_3)\text{Cl}$ might drive the reaction toward **Au11**–**8**. CH_2Cl_2 was used as a solvent to ensure that the gold precursor and the product remained soluble. A substoichiometric amount of NaBH_4 (only 0.25 mol equiv) was introduced as an ethanol solution into the CH_2Cl_2 solution of the precursor to initiate the reaction. **Au11**–**8** was obtained as the primary product prior to purification. A significant amount of unreacted starting material was recovered from the reaction mixture due to the low concentration of reducing agent. Silica gel chromatography removed all other products and the unreacted AuPPh_3Cl to provide 38% yield of **Au11**–**8**. Efforts to increase the conversion of AuPPh_3Cl to **Au11**–**8** by increasing the equivalents of reductant led to production of **Au11**–**7**.

We hypothesized that increasing the amount of reductant even more might lead to a larger percentage of **Au11**–**7** given that the traditional synthesis of the clusters led to the formation of both forms of undecagold and decreasing the amount of reductant produced mostly **Au11**–**8**. THF was used to increase the solubility of both AuPPh_3Cl and the reducing agent. Using THF as the main solvent and a 5-fold excess of NaBH_4 led to the formation of only the **Au11**–**7** cluster. Typical yields range from 65 to 70% after purification.

Differences in Ligation Result in Markedly Different Ligand Exchange Reactivity. Once pure samples of the two forms of undecagold were reproducibly prepared and their structures and spectral features determined, we investigated the differences in reactivity between the two forms. In order to determine whether the differences in reactivity were due to the ligation of the cluster, all other reaction conditions were kept constant. We used conditions originally reported for exchanges involving **Au11**–**8**: a biphasic reaction involving water and chloroform phases, 55 °C bath temperature, and 10 equiv of ligand. Glutathione was used in both cases to eliminate differences due to the structure of the exchanging ligands. Reactions were run under an N_2 atmosphere to minimize oxidation of the ligand.

The difference in reactivity between the two forms is evident from the colors of the aqueous phases (Figure 4) at the end of

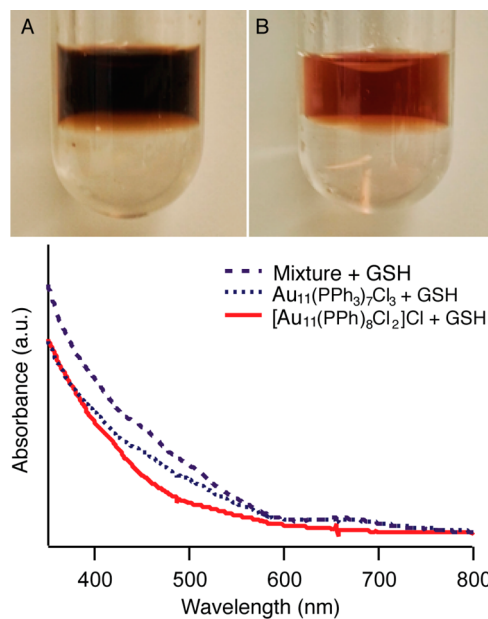


Figure 4. Photos and UV–visible spectra of the products of the biphasic ($\text{CHCl}_3/\text{H}_2\text{O}$) ligand exchange reactions between the two forms of undecagold and glutathione. The photos show visible differences in color (brown vs orange) in the water layer after ligand exchange with $\text{Au}_{11}(\text{PPh}_3)_7\text{Cl}_3$ (A) and $[\text{Au}_{11}(\text{PPh}_3)_8\text{Cl}_2]\text{Cl}$ (B). The UV–visible spectra show increased absorbance in the 600–700 nm region for the samples that contained $\text{Au}_{11}(\text{PPh}_3)_7\text{Cl}_3$.

the exchange reaction. When **Au11**–**7** is used as the starting material a brown solution results, and when **Au11**–**8** is used as the starting cluster a brown-orange color results. There is a noticeable absorbance peak in the UV–visible spectra around 670 nm for Au:SG clusters synthesized from **Au11**–**7** and from the mixture of **Au11**–**7** and **Au11**–**8**. This absorbance peak is characteristic of the $\text{Au}_{25}(\text{SG})_{18}$ cluster.^{24,47} It is significant that there is no such characteristic peak present when **Au11**–**8** is

used as the starting material. The absorbance spectra suggest that $\text{Au}_{25}(\text{SG})_{18}$ clusters are formed when **Au11-7** is present in the starting material but not formed when purified **Au11-8** is used. The formation and stability of the glutathione-exchanged product were monitored by UV-visible spectroscopy (see Supporting Information). Upon incubation in the reaction mixture over the course of 24 h, some of the clusters formed during exchange with **Au11-8** became unstable, yielding a white precipitate that is likely a $\text{Au}(\text{I})$ -alkanethiol polymer.⁴⁸ In contrast, $\text{Au}_{25}(\text{GS})_{18}$ clusters synthesized from **Au11-7** were stable in the reaction mixture for more than 24 h.

The ligand exchange products were analyzed by electrospray ionization mass spectrometry (ESI-MS) and polyacrylamide gel electrophoresis (PAGE). The mass spectra of all three glutathione-protected clusters synthesized are shown in Figure 5A. The peak with $m/z = 1740.5$ that corresponds to the

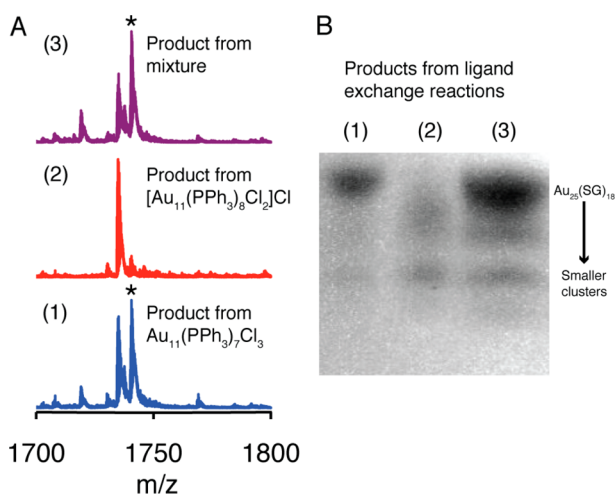


Figure 5. Analysis of reaction products of ligand exchange between glutathione and $\text{Au}_{11}(\text{PPh}_3)_7\text{Cl}_3$ (1), $[\text{Au}_{11}(\text{PPh}_3)_8\text{Cl}_2]\text{Cl}$ (2), and a mixture of the two (3). High-resolution ESI spectra (A) exhibit a peak at $m/z = 1740.5$ corresponding to a molecular ion ($\text{Au}_{25}(\text{GS})_{18}$ as the 6-plus ion) resulting from Au_{25} in the products from both reactions containing $\text{Au}_{11}(\text{PPh}_3)_7\text{Cl}_3$. Gel electrophoresis results (B) also suggest the presence of Au_{25} in the samples resulting from $\text{Au}_{11}(\text{PPh}_3)_7\text{Cl}_3$ and the mixture.

molecular ion $\text{Au}_{25}(\text{GS})_{18}$ (for the 6-plus species)²⁴ is present in the mass spectra obtained for products synthesized from **Au11-7** or from the mixture. This molecular ion is not observed when purified **Au11-8** is used as a starting material. Gel electrophoresis analysis (Figure 5B) was carried out on the purified $\text{Au}:\text{SG}$ clusters synthesized from **Au11-7** (1), **Au11-8** (2), and the mixture (3). The samples containing the slowest moving bands are the products obtained from **Au11-7** and from the mixture; these samples were found to contain $\text{Au}_{25}(\text{SG})_{18}$ clusters by ESI-MS. These bands are not present when **Au11-8** is used in the ligand exchange.

Taken together, the optical studies, gel electrophoresis, and mass spectrometry results suggest that glutathione exchange with **Au11-7** or mixtures including **Au11-7** leads to core growth and the production of $\text{Au}_{25}(\text{GS})_{18}$ as the major cluster species. Even small amounts of **Au11-7** in the mixture lead to the production of predominately $\text{Au}_{25}(\text{GS})_{18}$. **Au11-8**, on the other hand, does not form $\text{Au}_{25}(\text{GS})_{18}$. Some smaller clusters are observed in both PAGE and ESI-MS analysis of all of the cluster samples that are likely due to some amount of

nanoparticle etching in the presence of excess ligand.⁴⁹ The same reactivity trends were observed for the ligand exchange reaction between trimethylammoniummethanethiol (TMAT) and **Au11-7** and **Au11-8** (see Supporting Information).

The More Stable Cluster (Au11-8) Does Not Form Au_{25} during Ligand Exchange. Two questions follow from these findings. First, why does the relatively small difference in ligand shell composition lead to remarkably different reactivities for the two clusters? Second, why does the presence of even small amounts of **Au11-7** lead to particle growth and the formation of Au_{25} ? We considered several alternative hypotheses regarding the cluster reactivity. Given that both of the cluster species correspond to closed electronic shell (eight-electron) cores within the superatom counting approach,²⁸ the differences are not likely due to electronic structural differences. It is possible that the difference in reactivity is directly related to cluster stability which, in turn, may be influenced by differences in the steric stabilization or increased core charge induced by the additional TPP in **Au11-8**. If **Au11-7** is less stable and readily coalesces to form larger nanoparticles, these may be etched back down to Au_{25} by the excess thiol ligand. This hypothesis is related to the mechanism suggested by Shichibu et al.²⁰ that involves sequential growth and dissolution of the cores. An alternative hypothesis is that the less dense ligand shell in **Au11-7** permits oligomerization of the clusters during the early stages of ligand exchange and that subsequent rearrangement, addition, or removal of gold atoms adopts the thermodynamically stable Au_{25} structure.⁵⁰ The extra phosphine in **Au11-8** might inhibit coalescence of the clusters containing a mixed ligand shell early in the exchange process and permit the thiols to fully replace the phosphines and chlorides to retain the core size.

During our work with **Au11-7** and **Au11-8**, we noticed unexpected, but remarkable, differences in the stability of these clusters. The **Au11-7** cluster decomposes rapidly in CH_2Cl_2 even at room temperature. In contrast, **Au11-8** clusters are stable under the same conditions for months. We hypothesized that the stability of the clusters would differ even more at the elevated temperatures often used for ligand exchange reactions. Thus, we investigated the stabilities and decomposition products of both undecagold clusters under the temperature and solvent conditions used during typical ligand-exchange reactions.

Figure 6 shows the ^1H NMR spectra of **Au11-8** and **Au11-7** clusters before and after heating in CHCl_3 . The solutions were held at 50°C for the specified time and then cooled to room temperature. After the solvent was removed, the products were dissolved in CD_2Cl_2 for NMR analysis. The signature peaks that persist in the **Au11-8** spectrum (Figure 6A) demonstrate that these clusters are relatively stable, even after 210 min of heating in CHCl_3 . The new peaks in this spectrum indicate that $\text{Au}(\text{PPh}_3)\text{Cl}$ is formed and suggest that only a small number of the clusters have decomposed. After heating, the spectrum of the **Au11-7** products (Figure 6B) shows only peaks from $\text{Au}(\text{PPh}_3)\text{Cl}$, and there are no remaining peaks from **Au11-7**. Thin layer chromatography confirms formation of AuPPh_3Cl salt along with some other gold-containing species. These data suggest that the clusters have completely decomposed after 150 min of heating. We can conclude that stability of these clusters is vastly different under traditional ligand exchange conditions and that **Au11-7** is much less stable than **Au11-8**.

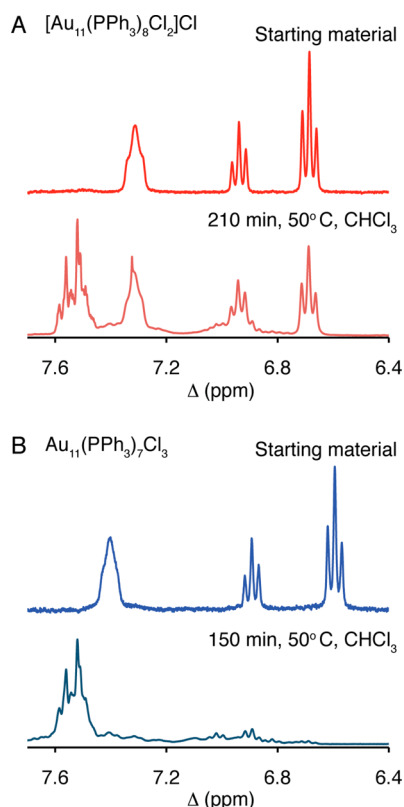


Figure 6. ^1H NMR spectra (recorded in CD_2Cl_2) of $[\text{Au}_{11}(\text{PPh}_3)_8\text{Cl}_2]\text{Cl}$ (A) and $\text{Au}_{11}(\text{PPh}_3)_7\text{Cl}_3$ (B) under ligand exchange reaction conditions that examine the relative thermal stability of the two forms. The lower spectra, obtained after keeping the undecagold starting materials in CHCl_3 solutions at elevated temperature for the time required for ligand exchange, show that $[\text{Au}_{11}(\text{PPh}_3)_8\text{Cl}_2]\text{Cl}$ is more stable at elevated temperature.

Other Reaction Parameters Have Less Influence than the Core Size: Optimized Ligand Exchange Conditions. The results described above show that cluster stability may be a key to the differences in ligand exchange reactivity of triphenylphosphine-stabilized undecagold. However, differences in the reaction conditions used in the previously reported studies could have influenced the exchange outcome. For example, under our original conditions, **Au11-8** was exchanged with 20 equiv of thiol ligands at $55\text{ }^\circ\text{C}$ (bath temperature) under air in CHCl_3 .¹⁸ Shichibu et al.²⁰ used a mixture of the undecagold forms (as indicated by starting UV–visible spectra), heated the reaction to 55 or $35\text{ }^\circ\text{C}$, and used larger amounts (430 or 60 equiv) of glutathione under both air and nitrogen atmospheres in the same solvent. It is possible that these other reaction parameters (particularly the temperature and the number of equivalents of incoming ligands), in addition to the nature of the starting clusters, might strongly influence the ligand exchange of the clusters.

To examine the impacts of thiol concentration, reaction temperature, and reaction time on the identity of the product, we monitored a series of ligand exchange reactions via UV–visible spectroscopy (see Supporting Information). First, an excess of glutathione ligand was introduced (430 equiv) to exchange reactions with each undecagold cluster (**Au11-8** and **Au11-7**) at different temperatures. It was found that, in general, such a large excess of glutathione does not lead to formation of $\text{Au}_{25}(\text{GS})_{18}$ at temperatures below $30\text{ }^\circ\text{C}$ if

Au11-8 is used as the starting material. However, when these solutions were kept under reaction conditions for 24 h, the exchanged clusters began to decompose, as evidenced by the precipitation of a white powder and a loss of color in the water layer. On the other hand, if **Au11-7** was used as the starting material, formation of $\text{Au}_{25}(\text{GS})_{18}$ was observed at $30\text{ }^\circ\text{C}$, as evidenced by increased absorbance at 670 nm. These larger ligand-exchanged clusters were stable under the reaction conditions for at least 24 h. When the temperature for the exchange was increased above $35\text{ }^\circ\text{C}$ and a large excess of glutathione was introduced (430 equiv), both undecagold starting materials produced $\text{Au}_{25}(\text{GS})_{18}$.

The structure of the undecagold precursor has the strongest effect on the outcome of the reaction but increasing reaction temperature can also lead to production of more $\text{Au}_{25}(\text{GS})_{18}$. Use of **Au11-8** in ligand-exchange reactions with low glutathione:undecagold ratios and low temperatures forms products that have smaller core sizes. In contrast, starting with **Au11-7** or the mixture, or increasing the reaction temperature leads primarily to Au_{25} regardless of the other conditions. These results suggest that product formation depends strongly on the stability of the precursor particle under the ligand-exchange reaction conditions.

Upon the basis of our evaluation of the influence of each reaction parameter, we have determined that the best conditions to preserve the small core size of undecagold during ligand exchange with water-soluble thiols include starting with **Au11-8** and conducting the exchange at $35\text{ }^\circ\text{C}$ with 60 or fewer equivalents of incoming ligand. Under these conditions, the ligand-exchange products do not show absorbance at 670 nm in the UV–visible spectrum and, therefore, suggest that Au_{25} is not formed and particles with small size are predominant. If Au_{25} is desired, one should start with **Au11-7** or the mixture or increase the reaction temperature during the ligand exchange.

CONCLUSION

We have discovered that two distinct forms of triphenylphosphine-stabilized undecagold exhibit significantly different ligand exchange reactivity even though they have the same Au core and nearly the same ligand shell. After isolating, characterizing and synthesizing each form, we monitored and evaluated the ligand exchange reactivities and cluster stabilities of both materials. Ligand exchange reactions carried out between glutathione and the two types of clusters revealed that exchange reactions of **Au11-7** or a mixture of **Au11-7** and **Au11-8** produce predominantly a larger cluster, Au_{25} . Analogous exchange reactions of pure **Au11-8** produced only smaller ($d_{\text{core}} \sim 0.8\text{ nm}$) particles. These results provide insight into the complex reactivity of Au_{11} and demonstrate for the first time that subtle changes in ligand shell composition can influence both particle stability and ligand exchange mechanisms.

This unexpected discovery provides insight into apparent discrepancies in the literature concerning the formulation of these clusters and the products of ligand exchange reactions conducted using the two forms. A reexamination of each of the previous reports, focusing on the optical spectra of the starting clusters and the reaction products, suggests that the primary reason for the apparent discrepancies is the differences in the undecagold species used in each case. Our investigations also inform how reaction conditions can be optimized to control the formation of the ligand-exchanged product. If the aim is to

preserve a small core size during exchange, one should employ **Au11–8**, keep the temperature at or below 50 °C, and use only a small excess of thiol (<60 equiv). If, on the other hand, the goal is to produce **Au25**, one should start with **Au11–7** or use temperatures in excess of 50 °C and use a large excess of thiol. The improved synthesis of the two forms and the optimized ligand exchange conditions make it possible to produce better defined materials for use in applications such as discrete tags for electron microscopy or well-defined catalyst precursors.

Reactions of Au clusters and nanoparticles appear to be influenced not only by the number of core atoms and identity of ligands but also by small variations in the arrangement of ligands. These findings suggest that the role of ligand shell composition in nanoparticle synthesis and ligand exchange reactions may be more complicated than previously expected. The fact that the core of **Au11–8** does not form **Au25** during exchange suggests that the larger number of bound PPh_3 ligands enhances stability and impedes transformations of this material or the intermediates formed during exchange. This may be a more general phenomenon within ligand exchange reactions of nanoparticles. If the intermediate (a partially exchanged nanoparticle) is stable, it is possible to obtain the kinetic product of ligand exchange that has the core intact. If the core becomes unstable with respect to coalescence, the product will be driven to lower energy, fused agglomerates. In the case of gold, these aggregates are, in turn, etched to the thermodynamically stable **Au25**. Our findings provide another example of how the complex reaction dynamics of nanoparticles, including etching/dissolution, renucleation, coalescence, size focusing and size/shape control are controlled by the ligand shell composition.

EXPERIMENTAL METHODS

Materials. Hydrogen tetrachloroaurate (99.9%, Strem Chemicals), triphenylphosphine (99%, Alfa Aesar), sodium borohydride (98%, Aldrich), L-glutathione reduced (>98%, Aldrich), 40% 19:1 acrylamide:bis(acrylamide) solution (Biorad), ammonium persulfate ($\geq 98\%$, Sigma), TEMED ($\geq 98\%$, tetramethylethylenediamine, Biorad), Tris Base ($\geq 99\%$, CalBioChem), hydrochloric acid ($\geq 99\%$, EMD Millipore), and glycine ($\geq 98.5\%$, J.T. Baker) were used as received. Sephadex G-50 Superfine was purchased from GE Healthcare. Silica gel (grade 62, 60–200 Mesh) was purchased from EMD. Thiocholine (*N,N,N*-trimethylammoniummethanethiol, TMAT) trifluoroacetate was synthesized according to the published procedure.^{51,52} Dichloromethane was distilled from calcium hydride prior to use. CHCl_3 was run through a plug of basic alumina prior to use. 18.2 M Ω -cm deionized water was used for all synthetic and purification processes. $\text{Au}(\text{PPh}_3)\text{Cl}$ was synthesized from HAuCl_4 and PPh_3 according to a known procedure.⁵³ All other reagents and solvents were purchased from Aldrich or Mallinckrodt and used as received.

Analytical Procedures. Nuclear magnetic resonance (NMR) spectra were collected at 25 °C on a Varian Unity Inova 300 MHz instrument equipped with a 4-channel probe (^{31}P , 121.43 MHz). For ^1H NMR spectroscopy, the spectra were collected from samples dissolved in CD_2Cl_2 or D_2O , and chemical shifts were referenced to the residual proton resonance of the solvent. For ^1H -decoupled ^{31}P NMR spectroscopy, the spectra were collected from nanoparticle samples dissolved in CD_2Cl_2 and referenced to 85% H_3PO_4 (external standard). UV–visible spectra (200–850 nm) of nanoparticle samples in CH_2Cl_2 were obtained on an Ocean Optics USB2000 spectrometer or Hewlett-Packard 8453 diode array instrument with a fixed slit width of 1 nm using 1 cm quartz cuvettes. Polyacrylamide gel electrophoresis was carried out by the same procedure reported in the literature.²⁴ The samples were dissolved in a 5% (v/v) aqueous glycerol solution (about 5 mg/mL) and 30 μL aliquots were loaded onto the gel. The electrospray ionization mass spectra of glutathione-protected clusters

were obtained on a AB SCIEX Triple ToF 5600 with a Shimadzu Nexera UPLC front end (positive mode). All samples (1 mg/mL in water) were analyzed as loop injections using 50:50 Acetonitrile/ H_2O /0.1% formic acid.

Single Crystal X-ray Characterization of Undecagold Clusters. The X-ray diffraction data for $\text{Au}_{11}(\text{PPh}_3)_7\text{Cl}_3$ were collected at 150(2) K using a Bruker Smart Apex II diffractometer and a synchrotron source (Advanced Light Source station 11.3.1, $\lambda = 0.77490$ Å). X-ray diffraction experiments for $[\text{Au}_{11}(\text{PPh}_3)_8\text{Cl}_2]\text{Cl}$ were carried out on a Bruker Smart Apex diffractometer at 153(2) K using $\text{MoK}\alpha$ radiation ($\lambda = 0.71073$ Å). Absorption corrections were applied by SADABS.⁵⁴ The dispersion values were calculated using WCCROMER Program in WinGX.⁵⁵ The structures were solved using direct methods with calculations of difference Fourier maps and refined with full-matrix least-squares methods based on F^2 . Non-hydrogen atoms were refined with anisotropic thermal parameters except those in a disordered solvent pentane molecule in $\text{Au}_{11}(\text{PPh}_3)_7\text{Cl}_3$. The H atoms in both structures were treated in calculated positions and refined in a rigid group model. In $\text{Au}_{11}(\text{PPh}_3)_7\text{Cl}_3$, one of the Ph-groups is disordered over two positions in the ratio 1:1 and as a result there is not full occupation for a CH_2Cl_2 solvent molecule (occupation factor = 0.5) contacted to this Ph-ring in the structure. There is another solvent molecule, pentane, that is disordered over two positions around an inversion center as well. The H atoms in the disordered pentane molecules were not taken into consideration in the refinement. The C atoms in this solvent molecule were refined with isotropic thermal parameters and restrictions on the C–C distances; the standard C–C distances were used as targets for corresponding C–C bonds. In the crystal structure of $[\text{Au}_{11}(\text{PPh}_3)_8\text{Cl}_2]\text{Cl}$, the Cl^- anion and solvent molecules (two CH_2Cl_2 and four $\text{CH}_3\text{CH}_2\text{OH}$) are disordered and form a disordered network via H-bonds. They were treated by SQUEEZE.⁵⁶ Correction of the X-ray data by SQUEEZE (801 electron/cell) is close to the required values (820 electron/cell). All calculations were performed using the SHELXTL (v. 6.10) package (Bruker AXS, Madison, WI).

Crystal data for $\text{Au}_{11}(\text{PPh}_3)_7\text{Cl}_3$: $\text{C}_{129}\text{H}_{112}\text{Au}_{11}\text{Cl}_4\text{P}_7$, $M_r = 4187.41$, $0.30 \times 0.04 \times 0.005$ mm, monoclinic, $P2_1/n$, $a = 17.864(3)$ Å, $b = 25.801(5)$ Å, $c = 26.912(5)$ Å, $\beta = 91.809(3)^\circ$, $V = 12398(4)$ Å³, $Z = 4$, $\rho_{\text{calcd}} = 2.243$ g cm^{−3}, $\mu = 16.329$ mm^{−1}, $2\theta_{\text{max}} = 58.20^\circ$, $T = 150(2)$ K, 211095 measured reflections, 25642 independent reflections [$R_{\text{int}} = 0.0586$], 1378 parameters, $R1$ and $wR2 = 0.0347$ and 0.0822 ($I > 2\sigma(I)$); 0.0573 and 0.0935 (all), $\text{GOF} = 1.069$ for all 25642 reflections, max/min residual electron density $+3.786/-1.766$ e Å^{−3}. Crystal data for $[\text{Au}_{11}(\text{PPh}_3)_8\text{Cl}_2]\text{Cl}$: $\text{C}_{154}\text{H}_{148}\text{Au}_{11}\text{Cl}_7\text{O}_4\text{P}_8$, $M_r = 4725.27$, $0.38 \times 0.35 \times 0.02$ mm, monoclinic, $P2_1/c$, $a = 22.5421(15)$ Å, $b = 18.0509(12)$ Å, $c = 34.593(2)$ Å, $\beta = 96.0670(10)^\circ$, $V = 13997(2)$ Å³, $Z = 4$, $\rho_{\text{calcd}} = 2.242$ g cm^{−3}, $\mu = 11.760$ mm^{−1}, $2\theta_{\text{max}} = 56.64^\circ$, $T = 153(2)$ K, 111788 measured reflections, 32960 independent reflections [$R_{\text{int}} = 0.0737$], 1486 parameters, $R1$ and $wR2 = 0.0484$ and 0.1045 ($I > 2\sigma(I)$); 0.0886 and 0.1144 (all), $\text{GOF} = 1.040$ for all 32960 reflections, max/min residual electron density $+3.923/-3.808$ e Å^{−3}.

Synthetic Procedures. Synthesis of Triphenylphosphine-Stabilized Undecagold Clusters. The synthesis of Au_{11} (producing a mixture of $\text{Au}_{11}(\text{PPh}_3)_7\text{Cl}_3$ (**Au11–7**) and $[\text{Au}_{11}(\text{PPh}_3)_8\text{Cl}_2]\text{Cl}$ (**Au11–8**)) followed the previously reported method.¹⁸ Briefly, 55 mL of absolute EtOH was added to a 100 mL round-bottom flask containing 1.00 g (2.02 mmol) $\text{Au}(\text{PPh}_3)\text{Cl}$. The cloudy white suspension was stirred while finely ground NaBH_4 (76 mg, 2.02 mmol) was added in small portions over 15 min (~ 1 addition/min). The solution color became yellow, light brown, and eventually dark brown over the course of the additions. After stirring at room temperature for 2 h, the mixture was poured into hexanes (1 L) and allowed to precipitate overnight (~ 20 h). The brown precipitate was collected on a medium porosity fritted funnel and washed with hexanes (4×15 mL), CH_2Cl_2 /hexanes (1:1, 4×15 mL), and CH_2Cl_2 /hexanes (3:1, 1×10 mL). The remaining orange/brown solid was dissolved and washed through the frit with CH_2Cl_2 (~ 40 mL). Crystallization by vapor diffusion of hexanes/ CH_2Cl_2 at 4 °C (described in the next section) produced a mixture of **Au11–7** as

orange needles and **Au11-8** as red plates (total product mass ~180 mg).

Crystallization of Triphenylphosphine-Stabilized Undecagold Clusters. The CH_2Cl_2 solution obtained after washing the product from the frit was divided ($3 \times \sim 13$ mL) and placed in 20 mL scintillation vials. The open vials were placed upright in 100 mL media bottles, and hexanes was carefully added to the bottles to prevent it from going into the vials. When the hexanes levels around the vials were above the CH_2Cl_2 levels but below the rims of the vials, the media bottles were capped and placed in the refrigerator at $\sim 4^\circ\text{C}$. Over 7–10 days, crystals of **Au11-7** and **Au11-8** formed, and light orange or colorless solution remained in the vials. The solution was removed with a pipet, and the crystals were washed with ~ 2 mL hexanes and isolated by filtration or decantation of wash solvent followed by evaporation of residual solvent under a stream of N_2 . After placing a mixed sample of crystals on filter paper under a microscope, the orange needles and red plates were mechanically separated using tweezers. The spectral data for each crystal type are as follows.

$\text{Au}_{11}(\text{PPh}_3)_7\text{Cl}_3$ (orange needles): ^1H NMR (300 MHz, 23°C , CD_2Cl_2) δ (ppm) = 7.40 (br t), 6.89 (dd), 6.59 (dd); ^{31}P NMR (121.43 MHz, 23°C , CD_2Cl_2 , vs H_3PO_4) δ (ppm) = 52.9; UV-vis (CH_2Cl_2) λ_{max} (nm) = 240, 308, 420.

$[\text{Au}_{11}(\text{PPh}_3)_8\text{Cl}_2]\text{Cl}$ (red plates): ^1H NMR (300 MHz, 23°C , CD_2Cl_2) δ (ppm) = 7.32 (br t), 6.94 (dd), 6.68 (dd); ^{31}P NMR (121.43 MHz, 23°C , CD_2Cl_2 , vs H_3PO_4) δ (ppm) = 52.2; UV-vis (CH_2Cl_2) λ_{max} (nm) = 240, 312, 416.

Crystallization of $[\text{Au}_{11}(\text{PPh}_3)_8\text{Cl}_2]\text{Cl}$ for X-ray Analysis. X-ray quality crystals of **Au11-8** were crystallized from a mixture of **Au11-7** and **Au11-8** (8:1 ratio by NMR, 24 mg). The mixture was dissolved in 5 mL of CH_2Cl_2 in a 20 mL scintillation vial. Octane was added until precipitation was observed (~ 3 mL). Then CH_2Cl_2 (10 mL) was added to dissolve all precipitate. The vial was capped with a septum and a needle that was open to the air. Over 7 days, the CH_2Cl_2 evaporated and left ~ 3 mL of solution. Red crystals formed on the sides of the vial, and light yellow solution that contained a few crystals remained in the vial. The solution was removed with a pipet, and the crystals were washed twice with 1 mL of octane. Most of the wash solvent was removed by pipet and residual solvent was evaporated under a stream of N_2 . Red plates removed from the wall of the vial were suitable for single crystal X-ray diffraction.

Crystallization of $\text{Au}_{11}(\text{PPh}_3)_7\text{Cl}_3$ for X-ray Analysis. Small X-ray quality crystals of **Au11-7** were obtained from the mixture of crystals produced during the vapor diffusion crystallization of the mixture from CH_2Cl_2 /hexane described in the section Crystallization of Triphenylphosphine-Stabilized Undecagold Clusters above. Attempts to produce larger single crystals were unsuccessful probably due to the instability of the cluster. Given the small size of the crystals, the structure determination of a single crystal was conducted at the Advanced Light Source.

Direct Synthesis of $[\text{Au}_{11}(\text{PPh}_3)_8\text{Cl}_2]\text{Cl}$. $\text{Au}(\text{PPh}_3)\text{Cl}$ (480 mg, 0.97 mmol) was dissolved in 20 mL of dichloromethane. A substoichiometric amount of NaBH_4 (10 mg, 0.27 mmol) dissolved in 3 mL of absolute ethanol was added to this solution in one portion under stirring at RT. The reaction progress was monitored by TLC ($\text{CH}_2\text{Cl}_2/\text{CH}_3\text{OH}$, v/v 5:0.5, the R_f of product is 0.4–0.5). The reaction mixture was stirred at RT for 24 h, and then solvents were evaporated. The residue was dissolved in a minimum amount of CH_2Cl_2 and the desired product was precipitated with 20 times this volume of pentane. The resulting mixture was centrifuged, and the supernatant was discarded. The residue was stirred with pentane (20 mL) and centrifuged, and the supernatant discarded. This procedure was repeated. The final solid was dissolved in CH_2Cl_2 , transferred to a round-bottom flask, and the solvent was evaporated to give the crude product. This material was dissolved in a minimum amount of CH_2Cl_2 and loaded onto a silica gel column packed with $\text{CH}_2\text{Cl}_2/\text{CH}_3\text{OH}$ (25:1 v/v). The product was eluted with $\text{CH}_2\text{Cl}_2/\text{CH}_3\text{OH}$ 10:1 to 5:1 mixture to give desired product (59 mg, 17% yield) and recovered gold salt (360 mg). The recovered starting material can be reduced to yield additional product through the following procedure. $\text{Au}(\text{PPh}_3)\text{Cl}$ (360 mg, 0.72 mmol) was dissolved in 15 mL of CH_2Cl_2 and used for

further reduction with NaBH_4 (8.4 mg, 0.22 mmol) in 2.5 mL of ethanol. The reaction and workup were carried out in the same manner as the first reaction. After chromatography, 68 mg of **Au11-8** was obtained bringing the overall yield to 127 mg (38%). Crystallization from CH_2Cl_2 /hexanes is recommended to obtain pure product. The spectral data for this material is the same as that described for the crystals above. Traces of $\text{Au}(\text{PPh}_3)\text{Cl}$ can influence the outcome of ligand exchange reactions, so it is important that the final undecagold cluster not contain any of this material.

Direct Synthesis of $\text{Au}_{11}(\text{PPh}_3)_7\text{Cl}_3$. $\text{Au}(\text{PPh}_3)\text{Cl}$ (500 mg, 1.01 mmol) was dissolved in 25 mL of THF. NaBH_4 (190 mg, 5.05 mmol) dissolved in 25 mL of absolute ethanol was added to this solution in one portion under stirring at RT. The clear colorless solution immediately became dark brown, and bubbles were observed. The reaction mixture was stirred at RT for 2 h and then was poured into pentane (500 mL) and allowed to precipitate for 2 h. The brown precipitate was collected on a medium-porosity fritted funnel and washed with hexanes (4×7.5 mL) and CH_2Cl_2 /hexanes (1:1, 4×7.5 mL). The remaining solid was then dissolved and washed through the frit into a tared vial or flask using 5 mL portions of CH_2Cl_2 and 2 min agitations until no color remained in the CH_2Cl_2 . The solvent was evaporated by rotary evaporation or flowing N_2 until constant mass of the desired product was obtained (250 mg, 66% yield). The spectral data for this material is the same as that described for the crystals above.

Ligand Exchange Procedures. Ligand Exchange of Triphenylphosphine-Stabilized Undecagold Clusters (Mixture of **Au11-8 and **Au11-7**) with Glutathione.** The synthesis of glutathione-stabilized Au clusters from a mixture of **Au11-7** and **Au11-8** followed the previously reported method for ligand exchange with **Au11-8**.¹⁸ An aqueous solution (13 mL) of glutathione (26 mg, 0.08 mmol) was added to a CHCl_3 solution (13 mL) of the mixture of **Au11-7** (15 mg, 0.004 mmol) and **Au11-8** (20 mg, 0.004 mmol) and deoxygenated with Ar for 2 min. The biphasic mixture was stirred rapidly at 50°C under N_2 for 3 h. After cooling to room temperature, the water layer was isolated in a separatory funnel and washed with CH_2Cl_2 (20 mL $\times 3$). The solution was concentrated to 1 mL using a rotary evaporator at room temperature and eluted on a Sephadex 50 column with water to give 20 mg of final product as a brown powder.

Ligand Exchange of $[\text{Au}_{11}(\text{PPh}_3)_8\text{Cl}_2]\text{Cl}$ with Glutathione. An aqueous solution (8 mL) of glutathione (15 mg, 0.05 mmol) was added to a CHCl_3 solution (8 mL) of **Au11-8** (20 mg, 0.005 mmol) and deoxygenated with Ar for 2 min. The biphasic mixture was stirred rapidly at 50°C under N_2 for 3 h. After cooling to room temperature, the water layer was isolated in a separatory funnel and washed with CH_2Cl_2 (20 mL $\times 3$). The solution was concentrated to 0.8 mL using a rotary evaporator at room temperature and eluted on a Sephadex 50 column with water to give 10 mg of final product as a brown-orange powder.

Ligand Exchange of $\text{Au}_{11}(\text{PPh}_3)_7\text{Cl}_3$ with Glutathione. An aqueous solution (10 mL) of glutathione (19 mg, 0.06 mmol) was added to a CHCl_3 solution (10 mL) of **Au11-7** (26 mg, 0.006 mmol) and deoxygenated with Ar for 2 min. The biphasic mixture was rapidly stirred at 50°C under N_2 for 3 h. After cooling to room temperature, the water layer was isolated in a separatory funnel and washed with CH_2Cl_2 (20 mL $\times 3$). The solution was concentrated to 1 mL using a rotary evaporator at room temperature and eluted on a Sephadex 50 column with water to give 10 mg of final product as a brown powder.

Stability Study Procedures. Stability Studies of Triphenylphosphine-Stabilized Undecagold Clusters. A CHCl_3 solution (5 mL) of **Au11-7** (10 mg, 0.002 mmol) was deoxygenated with Ar for 2 min and stirred at 50°C under N_2 for 150 min. The solution was cooled to room temperature, and the solvent was evaporated. The solid was redissolved in CH_2Cl_2 , and the solvent was evaporated for a second time to reduce the chloroform signal in the ^1H NMR spectrum. Finally, the sample was dissolved in CD_2Cl_2 , and the ^1H NMR was recorded. This process was repeated using **Au11-8** except that the solution was stirred at 50°C under N_2 for 210 min. The time was the only variable that was changed during these experiments.

■ ASSOCIATED CONTENT

■ Supporting Information

Additional characterization data (TEM, ^1H and ^{31}P NMR and UV–visible spectra) for $\text{Au}_{11}(\text{PPh}_3)_7\text{Cl}_3$ and $[\text{Au}_{11}(\text{PPh}_3)_8\text{Cl}_2]\text{Cl}$; UV–visible spectra of ligand exchange products at different times, temperatures, and with different ligands; and detailed synthetic procedures for ligand-exchanged clusters. This material is available free of charge via the Internet at <http://pubs.acs.org>.

■ AUTHOR INFORMATION

Corresponding Author

hutch@uoregon.edu

Present Address

‡ Chem11, LLC, 1672 East 23rd Avenue, Eugene, Oregon 97403, United States.

Author Contributions

† L. C. McKenzie and T. O. Zaikova contributed equally.

Notes

The authors declare no competing financial interest.

■ ACKNOWLEDGMENTS

We thank J. Purcell and B. L. Baldock for assistance with PAGE analysis; E. Healy, L. Zakharov and S. Teat for assistance collecting and analyzing X-ray diffraction data; J. T. Morré for assistance obtaining mass spectral data; and J. C. Scotland and M. L. Jespersen for helpful discussion. This work was supported by the Air Force Research Laboratory (under Agreement Number FA8650-05-1-5041). L.C.M. acknowledges support from the National Science Foundation IGERT Program under Grant No. DGE-0549503. The Center for Advanced Materials Characterization in Oregon (CAMCOR) is supported by the W. M. Keck Foundation, the M. J. Murdock Charitable Trust, the Oregon Nanoscience and Microtechnologies Institute and the University of Oregon. The Biomolecular Mass Spectrometry Core of the Environmental Health Sciences Core Center at Oregon State University is supported, in part, by Award Number P30ES000210 from the National Institute of Environmental Health Sciences (NIEHS), National Institutes of Health (NIH). The Advanced Light Source is supported by the Director, Office of Science, Office of Basic Energy Sciences, of the U.S. Department of Energy under Contract No. DE-AC02-05CH11231.

■ REFERENCES

- (1) Dahl, J. A.; Maddux, B. L. S.; Hutchison, J. E. *Chem. Rev.* **2007**, *107*, 2228.
- (2) Warner, M. G.; Hutchison, J. E. Synthesis and Assembly of Functionalized Gold Nanoparticles. In *Functionalization and Surface Treatment of Nanoparticles*; Baraton, M.-L., Ed.; American Scientific Publishers: Los Angeles, 2003; p 67.
- (3) Daniel, M.-C.; Astruc, D. *Chem. Rev.* **2003**, *104*, 293.
- (4) Erathodiyil, N.; Ying, J. Y. *Acc. Chem. Res.* **2011**, *44*, 925.
- (5) Saha, K.; Agasti, S. S.; Kim, C.; Li, X.; Rotello, V. M. *Chem. Rev.* **2012**, *112*, 2739.
- (6) Zhao, P.; Li, N.; Astruc, D. *Coord. Chem. Rev.* **2013**, *257*, 638.
- (7) Carageorgheopol, A.; Chechik, V. *Phys. Chem. Chem. Phys.* **2008**, *10*, 5029.
- (8) Heinecke, C. L.; Ni, T. W.; Malola, S.; Mäkinen, V.; Wong, O. A.; Häkkinen, H.; Ackerson, C. J. *J. Am. Chem. Soc.* **2012**, *134*, 13316.
- (9) Woehrle, G. H.; Brown, L. O.; Hutchison, J. E. *J. Am. Chem. Soc.* **2005**, *127*, 2172.
- (10) Woehrle, G. H.; Hutchison, J. E. *Inorg. Chem.* **2005**, *44*, 6149.
- (11) Brown, L. O.; Hutchison, J. E. *J. Am. Chem. Soc.* **1997**, *119*, 12384.
- (12) McPartlin, M.; Mason, R.; Malatesta, L. *J. Chem. Soc. D* **1969**, 334.
- (13) Malatesta, L.; Naldini, L.; Simonetta, G.; Cariati, F. *Coord. Chem. Rev.* **1966**, *1*, 255.
- (14) Grant, C. D.; Schwartzberg, A. M.; Yang, Y.; Chen, S.; Zhang, J. *Z. Chem. Phys. Lett.* **2004**, *383*, 31.
- (15) Bartlett, P. A.; Bauer, B.; Singer, S. J. *J. Am. Chem. Soc.* **1978**, *100*, 5085.
- (16) Jahn, W. *J. Struct. Biol.* **1999**, *127*, 106.
- (17) Safer, D.; Hainfeld, J.; Wall, J. S.; Reardon, J. E. *Science* **1982**, *218*, 290.
- (18) Woehrle, G. H.; Warner, M. G.; Hutchison, J. E. *J. Phys. Chem. B* **2002**, *106*, 9979.
- (19) This is the bath temperature. The reaction temperature is typically 5 °C lower.
- (20) Shichibu, Y.; Negishi, Y.; Tsukuda, T.; Teranishi, T. *J. Am. Chem. Soc.* **2005**, *127*, 13464.
- (21) Shichibu, Y.; Negishi, Y.; Watanabe, T.; Chaki, N. K.; Kawaguchi, H.; Tsukuda, T. *J. Phys. Chem. C* **2007**, *111*, 7845.
- (22) Yang, Y.; Chen, S. *Nano Lett.* **2003**, *3*, 75.
- (23) Hadley, A.; Aikens, C. M. *J. Phys. Chem. C* **2010**, *114*, 18134.
- (24) Negishi, Y.; Nobusada, K.; Tsukuda, T. *J. Am. Chem. Soc.* **2005**, *127*, 5261.
- (25) Gautier, C.; Bürgi, T. *J. Am. Chem. Soc.* **2008**, *130*, 7077.
- (26) Spivey, K.; Williams, J. I.; Wang, L. *Chem. Phys. Lett.* **2006**, *432*, 163.
- (27) Cariati, F.; Naldini, L. *Inorg. Chim. Acta* **1971**, *5*, 172.
- (28) Walter, M.; Akola, J.; Lopez-Acevedo, O.; Jadzinsky, P. D.; Calero, G.; Ackerson, C. J.; Whetten, R. L.; Gronbeck, H.; Häkkinen, H. *Proc. Natl. Acad. Sci. U. S. A.* **2008**, *105*, 9157.
- (29) Bergeron, D. E.; Hudgens, J. W. *J. Phys. Chem. C* **2007**, *111*, 8195.
- (30) Nunokawa, K.; Onaka, S.; Ito, M.; Horibe, M.; Yonezawa, T.; Nishihara, H.; Ozeki, T.; Chiba, H.; Watase, S.; Nakamoto, M. *J. Organomet. Chem.* **2006**, *691*, 638.
- (31) Nunokawa, K.; Onaka, S.; Yamaguchi, T.; Ito, T.; Watase, S.; Nakamoto, M. *Bull. Chem. Soc. Jpn.* **2003**, *76*, 1601.
- (32) Bellon, P.; Manassero, M.; Sansoni, M. *J. Chem. Soc., Dalton Trans.* **1972**, 1481.
- (33) Copley, R. C. B.; Mingos, D. M. P. *J. Chem. Soc., Dalton Trans.* **1996**, 479.
- (34) Schulz-Dobrick, M.; Jansen, M. *Z. Anorg. Allg. Chem.* **2007**, *633*, 2326.
- (35) Albano, V. G.; Bellon, P. L.; Manassero, M.; Sansoni, M. *J. Chem. Soc. D* **1970**, 1210.
- (36) Guttrath, B. S.; Englert, U.; Wang, Y.; Simon, U. *Eur. J. Inorg. Chem.* **2013**, *2013*, 2002.
- (37) Anderson, D. P.; Alvino, J. F.; Gentleman, A.; Qahtani, H. A.; Thomsen, L.; Polson, M. I. J.; Metha, G. F.; Golovko, V. B.; Andersson, G. G. *Phys. Chem. Chem. Phys.* **2013**, *15*, 3917.
- (38) Vollenbroek, F. A.; Van den Berg, J. P.; Van der Velden, J. W. A.; Bour, J. J. *Inorg. Chem.* **1980**, *19*, 2685.
- (39) Billings, S. B.; Mock, M. T.; Wiacek, K.; Turner, M. B.; Kassel, W. S.; Takeuchi, K. J.; Rheingold, A. L.; Boyko, W. J.; Bessel, C. A. *Inorg. Chim. Acta* **2003**, *355*, 103.
- (40) Hainfeld, J. F. Undecagold-Antibody Method. In *Colloidal Gold: Principles, Methods, and Applications*; Hayat, M. A., Ed.; Academic Press: San Diego, 1989; Vol. 2, p 415.
- (41) Hall, K. P.; Mingos, D. M. P. Homo- and Heteronuclear Cluster Compounds of Gold. In *Progress in Inorganic Chemistry*; John Wiley & Sons, Inc.: Hoboken, NJ, 1984; p 237.
- (42) Coffey, J. L.; Shapley, J. R.; Drickamer, H. G. *Inorg. Chem.* **1990**, *29*, 3900.
- (43) Mingos, D. M. *Gold Bull.* **1984**, *17*, 5.
- (44) Vollenbroek, F. A.; Bour, J. J.; van der Veden, J. W. A. *Recl. Trav. Chim. Pays-Bas* **1980**, *99*, 137.

- (45) Hagen, A. P.; Vollenbroek, F. A.; Velden, J. W. A. V. D.; Bour, J. J.; Steggerda, J. J. Gold Cluster Compounds Containing the Au₃, Au₄, Au₅, Au₆, Au₇, Au₈, Au₉, Au₁₁, Au₁₃ and Au₅₅, Cores. In *Inorganic Reactions and Methods*; John Wiley & Sons, Inc.: Hoboken, NJ, 1991; p 339.
- (46) Bellon, P. L.; Cariati, F.; Manassero, M.; Naldini, L.; Sansoni, M. *J. Chem. Soc. D* **1971**, 1423.
- (47) Zhu, M.; Eckenhoff, W. T.; Pintauer, T.; Jin, R. *J. Phys. Chem. C* **2008**, *112*, 14221.
- (48) Shichibu, Y.; Negishi, Y.; Tsunoyama, H.; Kanehara, M.; Teranishi, T.; Tsukuda, T. *Small* **2007**, *3*, 835.
- (49) Jin, R.; Qian, H.; Wu, Z.; Zhu, Y.; Zhu, M.; Mohanty, A.; Garg, N. *J. Phys. Chem. Lett.* **2010**, *1*, 2903.
- (50) Negishi, Y.; Chaki, N. K.; Shichibu, Y.; Whetten, R. L.; Tsukuda, T. *J. Am. Chem. Soc.* **2007**, *129*, 11322.
- (51) Warner, M. G.; Hutchison, J. E. *Nat. Mater.* **2003**, *2*, 272.
- (52) Kim, K.-T.; Zaikova, T.; Hutchison, J. E.; Tanguay, R. L. *Toxicol. Sci.* **2013**, *133*, 275.
- (53) Braunstein, P.; Lehner, H.; Matt, D. *Inorg. Synth.* **1990**, *27*, 218.
- (54) Sheldrick, G. M. *SHELXTL v. 5.10, Structure Determination Software Suite*; Bruker AXS: Madison, WI, 1998.
- (55) Kissel, L.; Pratt, R. H. *Acta Crystallogr., Sect. A: Found. Crystallogr.* **1990**, *A46*, 170.
- (56) Van der Sluis, P.; Spek, A. L. *Acta Crystallogr., Sect. A: Found. Crystallogr.* **1990**, *A46*, 194.